

See discussions, stats, and author profiles for this publication at: <https://www.researchgate.net/publication/6386391>

First-Principles Thermochemistry for the Production of TiO_2 from TiCl_4

ARTICLE *in* THE JOURNAL OF PHYSICAL CHEMISTRY A · JUNE 2007

Impact Factor: 2.69 · DOI: 10.1021/jp0661950 · Source: PubMed

CITATIONS

36

READS

166

4 AUTHORS, INCLUDING:



Richard Henry West

Northeastern University

30 PUBLICATIONS 394 CITATIONS

SEE PROFILE



Markus Kraft

University of Cambridge

213 PUBLICATIONS 3,035 CITATIONS

SEE PROFILE

First-Principles Thermochemistry for the Production of TiO₂ from TiCl₄Richard H. West,[†] Gregory J. O. Beran,[‡] William H. Green,[‡] and Markus Kraft^{*,†}

Department of Chemical Engineering, University of Cambridge, Cambridge CB2 3RA, U.K., and Massachusetts Institute of Technology, 77 Massachusetts Avenue, Cambridge, Massachusetts 02139

Received: September 21, 2006; In Final Form: February 15, 2007

Despite the industrial importance of the process, the detailed chemistry of the high-temperature oxidation of titanium tetrachloride (TiCl₄) to produce titania (TiO₂) nanoparticles remains unknown, partly due to a lack of thermochemical data. This work presents the thermochemistry of many of the intermediates in the early stages of the mechanism, computed using quantum chemistry. The enthalpies of formation and thermochemical data for TiOCl, TiOCl₂, TiOCl₃, TiO₂Cl₂, TiO₂Cl₃, Ti₂O₂Cl₃, Ti₂O₂Cl₄, Ti₂O₃Cl₂, Ti₂O₃Cl₃, Ti₃O₄Cl₄, and Ti₅O₆Cl₈ were calculated using density functional theory (DFT). The use of isodesmic and isogyric reactions was shown to be important for determining standard enthalpy of formation ($\Delta_f H_{298K}^\circ$) values for these transition metal oxychloride species. TiOCl₂, of particular importance in this mechanism, was also studied with CCSD(T) and found to have $\Delta_f H_{298K}^\circ = -598 \pm 20$ kJ/mol. Finally, equilibrium calculations were performed to identify which intermediates are likely to be most prevalent in the high temperature industrial process, and as a first attempt to identify the size of the critical nucleus.

1. Introduction

Titanium dioxide is currently produced at a rate over 4 million tons per year; half is used in paint, a quarter in plastics such as carrier bags and refrigerator doors, and most of the rest in paper, synthetic fibers, and ceramics. It is also used as a catalyst support and photocatalyst. The preferred production method is the chloride process, during which purified titanium tetrachloride is oxidized at high temperatures (1500–2000 K) and pressures (~300 kPa) in a pure oxygen plasma or flame to produce TiO₂ nanoparticles. The overall stoichiometry of this oxidation process is



Current reactor designs feature multiple feed points with independently controlled feed rates and pre-heat temperatures. Experimental optimization of such a system is incremental and costly. Although the chloride process is a mature technology, which has been used in industry since 1958, understanding of the gas-phase reactions of TiCl₄ oxidation remains incomplete.¹

A detailed kinetic model would ease the optimization of existing reactors as well as the development of new ones. Understanding the fundamentals of the chloride process for titania production may also contribute to the development of new processes for the industrial production of other powders for manufacture of electronic or structural ceramics.

Over the past 2 decades excellent kinetic models for silicon CVD chemistry have been developed,^{2,3} based on the fundamental thermochemistry of SiH₃Cl reactive intermediates from quantum chemistry.^{4,5} In an analogous way, the present work endeavors to provide the fundamental thermochemistry needed to allow the future development of kinetic models for systems involving titanium, oxygen, and chlorine.

Over the years, various mechanisms have been proposed to describe TiCl₄ oxidation. Pratsinis et al.⁶ proposed a mechanism in which TiCl₄ decomposes to TiCl_z radicals ($z < 4$) via thermal decomposition and abstraction reactions. These radicals are then oxidized to various TiO_yCl_z oxychlorides ($y \leq 2$, $z < 4$). The oxychlorides then dimerize to form Ti_xO_yCl_z ($x = 2$, $y \leq 4$) before reacting to yield species with $x > 2$, with subsequent reactions resulting in (TiO₂)_n nanoparticles ($n \gg 100$). Like Pratsinis, Karlemo et al.¹ proposed a mechanism via oxychloride intermediates, specifically TiOCl₂, which they found in detectable quantities. Despite these proposed mechanisms, no detailed simulations have been attempted due to a lack of thermochemical data for the intermediate species.

Experimentally, the only oxychloride intermediate to have been observed directly is TiOCl₂.^{1,7} Its presence at detectable levels suggests that it is likely to play an important role in the mechanism. Yet, the only thermochemical data currently available for TiOCl₂ and TiOCl, which are from the NIST JANAF Thermochemical Tables,⁸ were estimated in 1963. Other reactive intermediates in the chloride process are even more poorly characterized. Given that current experimental techniques cannot easily provide detailed thermochemical information for such short-lived reactive intermediates, quantum calculations provide a useful complementary tool.

Quantum calculations have previously been applied to titanium oxide species, particularly in the context of nanoclusters. Albaret et al.⁹ have studied Ti_nO_{2n+m} clusters ($n = 1-3$, $m = 0, 1$) using pseudopotential plane-wave density functional theory (DFT), and Woodley et al.¹⁰ recently used DFT to study the minimum energy structures of small (TiO₂)_n clusters ($n = 1-8$). While these studies shed light on the electronic and structural properties of titania nanoclusters, chlorine-free molecules are not part of the mechanisms proposed by Pratsinis or Karlemo and are unlikely to play an important role as intermediates in the chloride process.^{1,6}

The aim of this work is to provide thermochemical data for some of the titanium oxychloride species (Ti_xO_yCl_z), which will

* To whom correspondence should be addressed. E-mail: mk306@cam.ac.uk. Fax: +44 (0)1223 334796. Telephone: +44 (0)1223 334777.

[†] Department of Chemical Engineering, University of Cambridge.

[‡] Massachusetts Institute of Technology.

enable the development of more detailed kinetic models of the combustion of titanium tetrachloride. The results from three DFT functionals are compared, giving some indication of the reliability of DFT for these transition metal oxychloride species.

As well as probably playing an important role in the TiCl_4 oxidation mechanism, TiOCl_2 is a useful reference species for calculating the enthalpies of many other species; it is therefore subjected to a more detailed analysis using coupled cluster CCSD(T), often called “the gold standard of quantum chemistry”.

Since the optical and catalytic properties of TiO_2 depend strongly on particle size, a major technological issue in this large-scale industrial process is precisely controlling the particle size distribution. The size distribution is expected to depend strongly on the particle nucleation rate, which is strongly related to the size of the critical nucleus. Here we perform equilibrium calculations to identify which intermediates are likely to be most prevalent in the high temperature industrial process, and as a first attempt to identify the size of the critical nucleus.

2. Methods

2.1. Quantum Calculations. Molecular geometries have been optimized and analytical harmonic frequencies calculated using three different DFT functionals: mPWPW91,^{11–13} B3LYP,¹⁴ and B97-1.¹⁵ It is useful to compare the results of different density functionals because the absence of significant disagreements between different types of functional suggests that their predictions are not pathological. mPWPW91 is a generalized gradient approximation (GGA) functional; the other two are hybrid functionals as they also contain some exact Hartree–Fock exchange. The B3LYP functional is included here for comparison as it is probably the most widely used functional. However, Boese et al.¹⁶ concluded that B97-1 is probably the best choice when it comes to using density functional hybrid calculations and speculated that the continued popularity of less accurate first-generation functionals such as B3LYP is sheer user inertia. All functionals were as implemented in the Gaussian 03 program package.¹⁷

The basis set for all reported DFT calculations was 6-311+G(d,p).¹⁷ This consists of the 6-311G basis set¹⁸ for oxygen; the McLean–Chandler (12s,9p) (621111,52111) “negative ion” basis set¹⁹ for chlorine; the Wachters–Hay all-electron basis set^{20,21} for titanium, using the scaling factors of Raghavachari and Trucks;²² and supplementary polarization functions and diffuse functions. Such a supplemented, triple- ζ basis set should be large enough to ensure that the basis set truncation error is comparable with, or smaller than, the inherent errors in the DFT.¹⁶

Some species, such as TiOCl_3 , could not be adequately described by the default settings in Gaussian, so the B3LYP and B97-1 calculations were repeated with less restrictive settings: spin restriction was removed to detect possible spin contamination in singlet species, symmetry constraints were lifted to allow symmetry-breaking Jahn–Teller type distortions, the integral grid was increased to a pruned (99,590) grid, and the geometry optimization convergence criteria were tightened. To establish the spin multiplicity of the ground state, the lowest-energy state of different spin multiplicity was also calculated in many cases.

Species required to evaluate the enthalpy of formation of TiOCl_2 were investigated in more detail. Geometry optimization and frequency analyses were performed with BPW91^{12,13,23} and PW91PW91^{12,13} in addition to the three DFT functionals described above. These additional GGA functionals both use

TABLE 1: Reactions Used to Evaluate Standard Enthalpies of Formation ($\Delta_f H^\circ_{298\text{K}}$) from Computed Absolute Enthalpies

species	type	reaction
TiOCl	isodesmic	$\text{TiOCl}_2^a + \text{TiCl}_3^b \rightleftharpoons \text{TiOCl} + \text{TiCl}_4^c$
TiOCl_2	isogyric	$\frac{1}{2}\text{TiCl}_4^c + \frac{1}{2}\text{TiO}_2^c \rightleftharpoons \text{TiOCl}_2$
TiOCl_3	anisogyric	$\text{TiCl}_4^c + \text{TiOCl}_2^a \rightleftharpoons \text{TiOCl}_3 + \text{TiCl}_3^b$
TiO_2Cl_3	isogyric	$\text{TiCl}_4^c + \text{OCIO}^c \rightleftharpoons \text{TiO}_2\text{Cl}_3 + \text{Cl}_2^c$
TiO_2Cl_2	anisogyric	$\text{TiCl}_2^b + \text{O}_2^c \rightleftharpoons \text{TiO}_2\text{Cl}_2$
$\text{Ti}_2\text{O}_2\text{Cl}_4$	isogyric	$2\text{TiOCl}_2^a \rightleftharpoons \text{Ti}_2\text{O}_2\text{Cl}_4$
$\text{Ti}_2\text{O}_2\text{Cl}_3$	isogyric	$2\text{TiOCl}_2^a + \text{TiCl}_3^b \rightleftharpoons \text{Ti}_2\text{O}_2\text{Cl}_3 + \text{TiCl}_4^c$
$\text{Ti}_2\text{O}_3\text{Cl}_3$	anisogyric	$2\text{TiOCl}_2^a + \text{TiOCl}_2^a \rightleftharpoons \text{Ti}_2\text{O}_3\text{Cl}_3 + \text{TiCl}_3^b$
$\text{Ti}_2\text{O}_3\text{Cl}_2$	isogyric	$2\text{TiOCl}_2^a + \text{TiOCl}_2^a \rightleftharpoons \text{Ti}_2\text{O}_3\text{Cl}_2 + \text{TiCl}_4^c$
$\text{Ti}_3\text{O}_4\text{Cl}_4$	isogyric	$2\text{TiOCl}_2^a + \text{TiO}_2^b \rightleftharpoons \text{Ti}_3\text{O}_4\text{Cl}_4$
$\text{Ti}_5\text{O}_6\text{Cl}_8$	isogyric	$6\text{TiOCl}_2^a \rightleftharpoons \text{Ti}_5\text{O}_6\text{Cl}_8 + \text{TiCl}_4^c$

^a Enthalpy of formation from this work. ^b Enthalpy of formation from Hildenbrand (1996).³⁷ ^c Enthalpy of formation from NIST-JANAF tables.⁸

the same PW91 correlation as mPWPW91, but with Becke’s exchange functional and the PW91 exchange functional respectively. Using B3LYP optimized geometries, single point coupled cluster CCSD(T) calculations were performed using the software GAMESS–UK version 7.^{24,25} This software can only perform spin restricted CCSD(T) calculations; however, this is not a problem in this case as none of the species studied with CCSD(T) preferred a spin unrestricted solution at the UB3LYP or UHF levels of theory.

Three different basis sets were used for the CCSD(T) calculations. For titanium the two smallest basis sets both used the LANL2 Hay and Wadt effective core potentials (ECPs), with the inner-valence forms used for transition metals.²⁶ Oxygen and chlorine were taken from 3-21G^{27,28} for the smallest basis set and 6-311G¹⁸ for the intermediate case. For the largest basis set calculations, the all-electron 6-311+G(d,p) basis set was used for all three elements, as with the DFT calculations. Only three small molecules (TiCl_4 , TiO_2 , and TiOCl_2) were calculated with the larger two basis sets due to the n^7 scaling of CCSD(T) and the limited computing resources available.

Vibrational frequencies were not calculated at the HF, MP2, CCSD, or CCSD(T) levels, so these enthalpies have been corrected with thermal contributions according to B97-1/6-311+G(d,p) frequencies and rotational constants.

2.2. Statistical Mechanics and Equilibrium Composition. Heat capacities (C_p), integrated heat capacities ($H(T) - H(0\text{ K})$), and entropies (S) were calculated for temperatures in the range 100–3000 K using the rigid rotator harmonic oscillator (RRHO) approximation, taking unscaled vibrational frequencies and rotational constants from the B97-1 calculations (see Table 4).

Polynomials in the NASA form²⁹ were fitted to $C_p(T)/R$, H° , and S° over the temperature ranges 100–1000 K and 1000–3000 K, constrained to ensure $C_p(T)$ and its first two derivatives matched at 1000 K. Using the fitted polynomials for $C_p(T)$, $H^\circ(T)$ and $S^\circ(T)$, the equilibrium composition as a function of temperature was calculated using the open source software Cantera.³⁰

2.3. Enthalpies of Formation: Isodesmic and Isogyric Reactions. The atomization energies reported in section 3.2 were found by subtracting the DFT-computed absolute energies of the component atoms in isolation from the absolute energies of the species computed at the same level of theory. Standard enthalpies of formation ($\Delta_f H^\circ_{298\text{K}}$) are found by relating the computed absolute enthalpies of the unknown species to those of other reference species with previously known standard enthalpies. Although a common choice for these reference species are the isolated atoms, this can lead to systematic errors in the DFT propagating to the final enthalpies; better results

TABLE 2: Atomization Energies at 0 K in kJ/mol with 6-311+G(d,p) Basis Set (DFT Calculations Include ZPE Correction)

species	spin state	mPWPW91	B3LYP	B97-1	lit.
TiO ₂	singlet	-1436	-1226	-1269	-1268 ^a
TiCl ₄	singlet	-1828	-1641	-1719	-1687 ^a
TiCl ₃	doublet	-1424	-1296	-1354	-1335 ^b
TiCl ₂	triplet	-974	-840	-921	-913 ^b
TiCl	quartet	-481	-428	-438	-405 ^b
TiOCl	doublet	-1231	-1085	-1127	-1074 ^a
TiOCl ₂	singlet	-1675	-1490	-1552	-1489 ^a
TiOCl ₃	doublet	-1838	-1627	-1694	
Ti ₂ Cl ₂	singlet	-1953	-1715	-1785	
Ti ₂ O ₂ Cl ₃	doublet	-2188	-1935	-2018	
Ti ₂ O ₂ Cl ₄	singlet	-3705	-3335	-3457	
Ti ₂ O ₂ Cl ₃	doublet	-3281	-2960	-3061	
Ti ₂ O ₃ Cl ₂	singlet	-3515	-3133	-3238	
Ti ₂ O ₃ Cl ₃	doublet	-3697	-3300	-3421	
Ti ₃ O ₄ Cl ₄	singlet	-5558	-5001	-5167	
Ti ₃ O ₆ Cl ₈	singlet		-8481	-8771	

^a NIST-JANAF tables.⁸ ^b Atomization enthalpy at 298 K based on Hildenbrand⁷ and the NIST-JANAF tables.⁸

TABLE 3: Enthalpies of Formation of TiOCl₂ Derived from the Isogyric Reaction Described in Table 1, Where HF, MP2, CCSD, and CCSD(T) Calculations Were Based on B3LYP/6-311+G(d,p) Geometries and Have Been Corrected for Thermal Contributions to Enthalpy Using B97-1/6-311+G(d,p) Frequencies

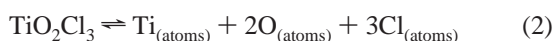
basis set	method	$\Delta_f H_{298K}^o$ ^a
LANL2 & 3-21G	lit. ^b	-546
	HF	-652
	MP2	-635
	CCSD	-636
	CCSD(T)	-620
LANL2 & 6-311G(d,p)	HF	-636
	MP2	-623
	CCSD	-623
	CCSD(T)	-609
6-311+G(d,p)	PW91PW91	-578
	BPW91	-579
	mPWPW91	-579
	B3LYP	-590
	B97-1	-591
	HF	-638
	MP2	-607
	CCSD	-610
	CCSD(T)	-598

^a kJ/mol. ^b NIST/JANAF tables.⁸

can usually be obtained using reference species that are more similar in terms of electronic structure to the unknown species.

Ideally the reference species are chosen such that they are linked to the unknown species via an isodesmic reaction, in which the type of the bonds broken are the same as the type of bonds formed. Because the products and reactants have similar electronic structures, systematic errors in the DFT are largely cancelled out.³¹ While less desirable than isodesmic reactions, isogyric reactions, which conserve the number of electron pairs in reactants and products, are still better than atomization reactions.^{32,33}

Reaction choice is particularly important with the titanium oxychloride species, as shown here with the radical TiO₂Cl₃. Calculation of standard enthalpy of formation from atomization energies is equivalent to using the reaction



Here a doublet reactant (one unpaired electron) is compared to three triplet and three doublet species (total of nine unpaired

electrons). Using this reaction to establish the standard enthalpy of formation with the 6-311+G(d,p) basis set, the mPWPW91, B3LYP, and B97-1 functionals give formation enthalpies for TiO₂Cl₃ of -865, -612, and -694 kJ/mol, respectively. This is a spread of 253 kJ/mol, far exceeding the expected accuracy of DFT calculations.¹⁶

Reliable enthalpies of formation are available for TiCl₃ and O₂; therefore, an alternative choice of reaction is



However, on the left-hand side is a doublet with the spin concentrated on the oxygen atoms, which are in the 2- oxidation state, and on the right is one doublet with the spin on the titanium and one triplet with the oxygen atoms in the ground oxidation state. Using this scheme to establish enthalpies changes the mPWPW91 value to -702 kJ/mol, a change of +163 kJ/mol relative to the atomization scheme. The B3LYP and B97-1 functionals give -648 and -657 kJ/mol, respectively, reducing the overall spread to 54 kJ/mol.

A third alternative reaction is



This reaction is isogyric, as there are 61 electron pairs and one unpaired electron on both the reactant and product sides, with one doublet and one singlet on each side of the reaction. Linking the absolute energies to standard values with this isogyric reaction places the standard enthalpy of formation of TiO₂Cl₃ at -734, -772, and -771 kJ/mol according to the mPWPW91, B3LYP, and B97-1 functionals respectively. The overall spread of 38 kJ/mol and the very close agreement of the latter two functionals adds confidence to the numbers achieved this way. The variation of up to 160 kJ/mol between reaction schemes shows both the importance of their choice and the challenge of obtaining a uniformly accurate treatment of these transition metal species with different spin states.³⁴

Because of the paucity of thermochemical data for transition metal oxychloride species, it was not possible to find isodesmic or isogyric reactions linking all the species studied in this work to species with reliable literature values for $\Delta_f H_{298K}^o$. However, any reaction that leaves some bonds intact is preferable to atomization. The reactions used to evaluate standard enthalpies of formation are shown in Table 1.

3. Results and Discussion

3.1. Geometries. Figure 1 shows the molecular geometries of the ground state of each molecule after optimization with B97-1/6-311+G(d,p).

At this level of theory, TiOCl₃ in a C_{3v} conformation has an imaginary frequency. This is due to a Jahn-Teller distortion, which results from a very low-lying first excited state (0.21 eV for the C_{3v} structure according to TDDFT with the B3LYP functional). The C_s geometry reported here is stable at this level of theory.

Two stable geometries for TiO₂Cl₂ were located. At the B97-1/6-311+G(d,p) level the isomer with a trigonal Ti center and a dangling -O-O has an electronic energy 201 kJ/mol higher than the structure with the distorted tetrahedral geometry reported here, in which the O atoms are both bonded to the Ti.

3.2. Atomization Energies. Although we have not used atomization reactions to calculate enthalpies of formation, we report atomization energies here to facilitate reproduction of our results. Table 2 shows the atomization energies for the

TABLE 4: Calculated Thermochemistry at 298 K

species	$\Delta_f H_{298K}^\circ$ kJ/mol	S_{298K}° J/mol K	rotational const. GHz	vibrational frequencies cm ⁻¹
TiOCl	-274 ^a	292	39.120, 2.9782, 2.7676	113, 398, 1036
TiOCl ₂	-598 ^b	335	5.4126, 1.7850, 1.3423	23.0, 113, 212, 378, 506, 1091
TiOCl ₃	-639	379	1.6461, 1.5723, 1.0712	77.1, 94.0, 116, 144, 155, 378, 469, 483, 669
TiO ₂ Cl ₂	-558	342	2.6652, 1.8968, 1.1982	110, 125, 149, 174, 384, 493, 658, 683, 966
TiO ₂ Cl ₃	-774	404	1.2747, 1.2687, 1.1039	33.0, 108, 127, 140, 147, 160, 389, 405, 470, 493, 549, 1229
Ti ₂ O ₂ Cl ₃	-1257	438	1.7164, 0.4549, 0.3859	14.1, 72.4, 82.7, 100, 140, 161, 273, 278, 393, 422, 495, 539, 695, 708, 760
Ti ₂ O ₂ Cl ₄	-1552	449	0.9517, 0.4544, 0.3262	40.4, 65.8, 91.6, 97.1, 102, 116, 152, 214, 294, 302, 398, 410, 489, 527, 539, 710, 731, 767
Ti ₂ O ₃ Cl ₂	-1331	402	1.6100, 0.7549, 0.5699	59.6, 101, 122, 142, 164, 256, 303, 335, 462, 488, 494, 707, 722, 776, 1065
Ti ₂ O ₃ Cl ₃	-1418	461	1.2145, 0.5034, 0.3813	44.0, 61.3, 89.0, 105, 108, 135, 159, 187, 293, 315, 330, 420, 504, 533, 690, 703, 732, 765
Ti ₃ O ₄ Cl ₄	-2301	538	0.8631, 0.1581, 0.1581	30.3, 31.9, 50.6, 85.3, 85.9, 87.8, 108, 138, 140, 163, 235, 239, 290, 291, 354, 439, 439, 444, 507, 508, 534, 709, 714, 717, 739, 765, 778
Ti ₅ O ₆ Cl ₈	-4011	823	0.1297, 0.0875, 0.0875	19.4, 20.8, 20.8, 28.5, 28.5, 39.0, 58.0, 61.9, 67.8, 77.8, 80.7, 83.8, 83.8, 99.3, 109, 109, 110, 129, 140, 141, 141, 220, 223, 223, 246, 246, 283, 321, 327, 327, 331, 371, 383, 429, 429, 484, 486, 486, 494, 499, 510, 510, 521, 555, 626, 754, 754, 823, 876, 881, 881

^a JANAF value: -244 kJ/mol (estimated in 1963). ^b Electronic energy from CCSD(T)/6-311+G(d,p) at B3LYP/6-311+G(d,p) geometry. Thermal contribution to enthalpy from B97-1/6-311+G(d,p) frequencies. JANAF value: -546 kJ/mol (estimated in 1963).

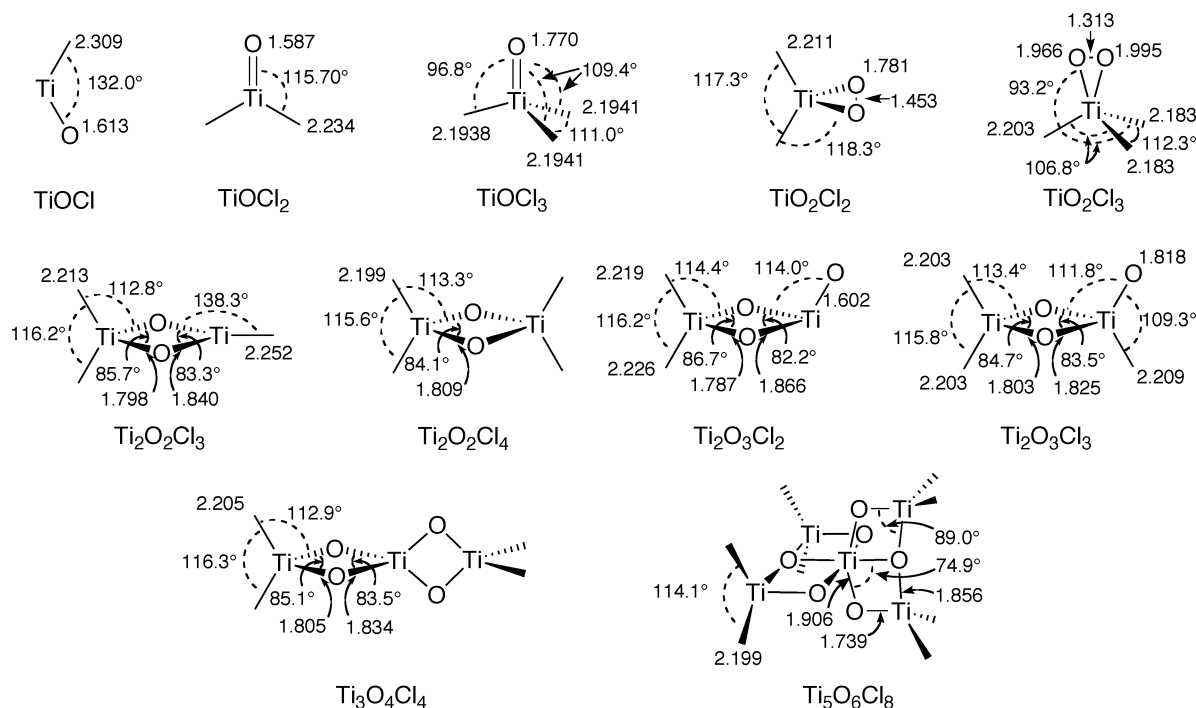


Figure 1. Molecular geometries after optimization with B97-1/6-311+G(d,p). Bond lengths are in Å, and unlabeled atoms are chlorine.

ground electronic state calculated with the 6-311+G(d,p) basis set using three DFT functionals: mPWPW91, B3LYP, and B97-1.

The lowest-energy states of different spin multiplicity from the ground states were of considerably higher energies. The smallest gap was for TiCl in which the doublet state is ~40 kJ/mol higher than the quartet state; all the other gaps were at least 100 kJ/mol.

3.3. TiOCl₂. As explained in the introduction, TiOCl₂ and the species required to find its enthalpy of formation (TiCl₄ and TiO₂), were subjected to a more detailed analysis using two additional DFT functionals as well as HF, MP2, and coupled cluster calculations. The enthalpies of formation derived from these calculations are reported in Table 3.

The MP2/CCSD/CCSD(T) results converge nicely with respect to basis set and increasing level of correlation treatment.

CCSD and MP2, which both include up to double excitations from the HF reference, agree very closely, lowering the enthalpy by 28–31 kJ/mol relative to HF/6-311+G(d,p). The additional perturbative inclusion of triple excitations in CCSD(T), though important, introduces a smaller correction, changing the energy by 9–12 kJ/mol from MP2 and CCSD in the 6-311+G(d,p) basis set. These results suggest that the correlation treatment is well-behaved with respect to systematic improvement, and it seems reasonable to expect that higher order excitations would not alter the enthalpy of formation by more than ~10 kJ/mol. The good agreements with B3LYP and B97-1 (8 and 7 kJ/mol lower, respectively) further inspire confidence in the predictions within this basis set.

Although a supplemented triple- ζ basis set is sufficient for DFT calculations,¹⁶ it is possible that the CCSD(T) calculations are limited by basis set truncation error and would benefit from

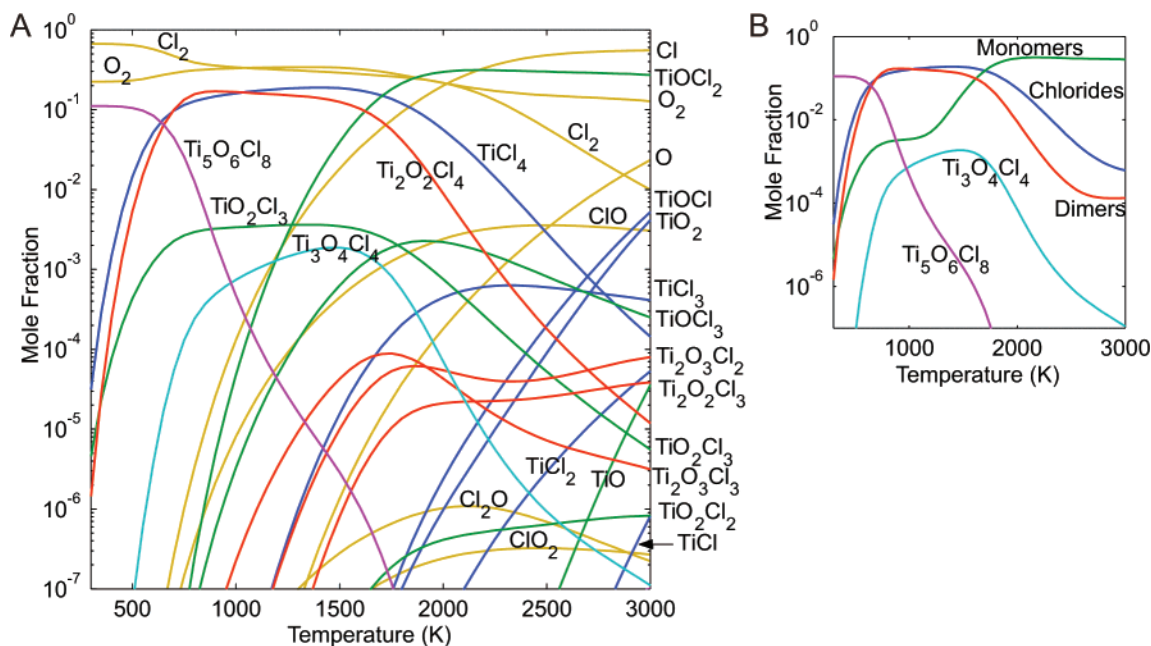


Figure 2. Computed equilibrium composition of a mixture initially containing 50 mol % TiCl_4 in O_2 , at 3 bar and 300–3000 K: (A) detailed composition; (B) summary with chlorides (TiCl_x), monomers (TiO_yCl_z), and dimers ($\text{Ti}_2\text{O}_y\text{Cl}_z$) grouped.

a larger basis set. Moving O and Cl from 3-21G, a poor double- ζ basis set, to 6-311G(d,p), a better triple- ζ basis set with polarization functions, lowers the enthalpy of TiOCl_2 by 11 kJ/mol for CCSD(T). A further 11 kJ/mol change occurs when the all-electron triple- ζ basis is used instead of the ECP for Ti and diffuse functions are added to all atoms. These relatively small changes in enthalpy suggest that basis set errors are not too large. Estimating a 10 kJ/mol error from basis set truncation and allowing 10 kJ/mol error from omitting higher order excitations, we think 20 kJ/mol is a reasonable estimate of the overall uncertainty.

On the basis of these calculations we recommend a value of $\Delta_f H_{298\text{K}}^\circ = -598 \pm 20$ kJ/mol for TiOCl_2 . The NIST/JANAF value of -546 kJ/mol, which apparently is an old estimate not based on any direct measurement, lies outside our estimated uncertainty, and so should be considered for revision. We have used the value calculated here (-598 kJ/mol) in deriving $\Delta_f H_{298\text{K}}^\circ$ values for other species in this paper.

3.4. Thermochemistry. The recommended standard entropies and enthalpies of formation at 298 K are given in Table 4 along with B97-1 frequencies. With the exception of TiOCl_2 the recommended enthalpies are based on the B97-1 functional, which is probably the most accurate.¹⁶ For TiOCl_2 the electronic energy is from the CCSD(T)/6-311+G(d,p) calculation based on the B3LYP geometry, with the thermal energy based on B97-1 frequencies reported here.

For most species the enthalpies derived from B3LYP calculations differed from the B97-1 enthalpies by less than 2 kJ/mol. The exceptions were the three species that were evaluated through anisodesmic reactions: TiOCl_3 , TiO_2Cl_2 , and $\text{Ti}_2\text{O}_3\text{Cl}_3$, for which the B3LYP enthalpies were respectively 15 kJ/mol lower, 22 kJ/mol higher, and 7 kJ/mol lower than the B97-1 enthalpies. While this close agreement increases confidence in the calculations, it is worth remembering that the actual error will be larger than this; B3LYP and B97-1 are both hybrid DFT functionals with some exact (HF) exchange and so behave similarly. MPWPW91, a pure DFT functional, gives enthalpies that differ from B97-1 by ~ 20 kJ/mol on average and as much as 59 kJ/mol for the anisodesmic reaction to find TiO_2Cl_2 . In addition to errors in the DFT calculations, errors in

the reference species enthalpies will propagate to the enthalpies that are derived from them.

3.5. Equilibrium Composition. Figure 2 shows the computed equilibrium composition of a gas initially comprising a stoichiometric mixture of TiCl_4 and O_2 , at a pressure of 3 bar, similar to that of the industrial process, and temperatures between 100 and 3000 K. The thermochemical data for TiOCl , TiOCl_2 , TiOCl_3 , TiO_2Cl_2 , TiO_2Cl_3 , $\text{Ti}_2\text{O}_2\text{Cl}_4$, $\text{Ti}_2\text{O}_3\text{Cl}_2$, $\text{Ti}_2\text{O}_3\text{Cl}_3$, $\text{Ti}_3\text{O}_4\text{Cl}_4$, and $\text{Ti}_5\text{O}_6\text{Cl}_8$, were taken from this work. Those for TiCl_4 , TiCl_3 , TiCl_2 , TiCl , Ti , TiO , TiO_2 , O , O_2 , O_3 , Cl , ClO , ClO_2 , Cl_2 , and Cl_2O were taken from the NASA database^{29,35} supplied with Cantera. All other species, including solid TiO_2 , were excluded from the simulation.

As anticipated, TiOCl_2 has the highest equilibrium concentration of all Ti_1 species except, below 1700 K, for the reactant TiCl_4 . Although less stable than TiOCl_2 , the other TiO_yCl_z species are no less important for the kinetic mechanism, because TiOCl_2 is unlikely to be formed directly from TiCl_2 radicals, instead proceeding via TiO_2Cl_2 or TiO_2Cl_3 from reaction with O_2 , or via TiOCl_3 from reaction with ClO . Because of the stability of TiOCl_2 relative to other reactive Ti_1 species, the most likely collision that leads to a Ti_2 species is between two TiOCl_2 molecules. The product of TiOCl_2 dimerization, $\text{Ti}_2\text{O}_2\text{Cl}_4$, is stable relative to the monomer at all temperatures below 1700 K, and is therefore likely to play an important role in the mechanism. $\text{Ti}_2\text{O}_2\text{Cl}_4$ can undergo chlorine abstraction and oxidation reactions to form other Ti_2 intermediates such as $\text{Ti}_2\text{O}_2\text{Cl}_3$, $\text{Ti}_2\text{O}_3\text{Cl}_2$, and $\text{Ti}_2\text{O}_3\text{Cl}_3$, so although these are less stable than $\text{Ti}_2\text{O}_2\text{Cl}_4$ at most temperatures, they may still feature in a detailed kinetic mechanism, much like the lesser TiO_yCl_z species.

Of the many possible Ti_3 species, we expect $\text{Ti}_3\text{O}_4\text{Cl}_4$ to be one of the more stable due to the double-oxygen bridge between each of the Ti atoms. However, the equilibrium concentration of this species is predicted to be lower than that of the dimer by at least an order of magnitude. This implies that the critical nucleus size, above which molecules grow irreversibly and can be safely treated as particles,³⁶ is larger than Ti_2 .

Below ~ 600 K the largest species in our simulation, $\text{Ti}_5\text{O}_6\text{Cl}_8$, is predicted to have the highest concentration of the

species containing titanium. This suggests that at low temperatures the critical nucleus size has five or fewer Ti atoms. However, at the high temperatures employed to speed the kinetics in the industrial process, the Ti_5 species is unstable relative to the reactants $TiCl_4 + O_2$, suggesting that the critical nucleus size is even larger under those conditions.

4. Conclusion

Quantum calculations were used to obtain thermochemical data, including standard entropies and enthalpies of formation, for some titanium oxychloride species, $Ti_xO_yCl_z$, many of which were not previously reported in the literature and are impossible to obtain with available experimental techniques. These thermochemical data will enable the development of more detailed kinetic models of the combustion of titanium tetrachloride to produce titanium dioxide. A comparison of the results from these calculations with the NIST and JANAF tables suggests that the literature values for $TiOCl_2$ should be revised.

Acknowledgment. The authors would like to thank the EPSRC and Huntsman TiOxide for the financial support of RHW through an Industrial CASE studentship. Additional financial support from the US National Science Foundation is gratefully acknowledged. WHG thanks Churchill College for a Bye Fellowship, which greatly facilitated this collaboration.

Supporting Information Available: Thermochemical tables and polynomial coefficients in NASA form for $C_p(T)$, $H^\circ(T)$, and $S^\circ(T)$ for the species $TiOCl$, $TiOCl_2$, $TiOCl_3$, TiO_2Cl_2 , TiO_2Cl_3 , $Ti_2O_3Cl_3$, $Ti_2O_3Cl_2$, $Ti_2O_2Cl_3$, $Ti_3O_4Cl_4$, $Ti_2O_2Cl_4$, and $Ti_5O_6Cl_8$. This material is available free of charge via the Internet at <http://pubs.acs.org>.

References and Notes

- (1) Karlemo, B.; Koukari, P.; Paloniemi, J. *Plasma Chem. Plasma Proc.* **1996**, *16*, 59–77.
- (2) Coltrin, M. E.; Kee, R. J.; Miller, J. A. *J. Electrochem. Soc.* **1986**, *133*, 1206–1213.
- (3) Coltrin, M. E.; Ho, P.; Moffat, H. K.; Buss, R. J. *Thin Solid Films* **2000**, *365*, 251–263.
- (4) Ho, P.; Coltrin, M. E.; Binkley, J. S.; Melius, C. F. *J. Phys. Chem.* **1985**, *89*, 4647–4654.
- (5) Ho, P.; Melius, C. F. *J. Phys. Chem.* **1995**, *99*, 2166–2176.
- (6) Pratsinis, S. E.; Bai, H.; Biswas, P.; Frenklach, M.; Mastrangelo, S. V. R. *J. Am. Ceram. Soc.* **1990**, *73*, 2158–2162.
- (7) Hildenbrand, D. L.; Lau, K. H.; Mastrangelo, S. V. R. *J. Phys. Chem.* **1991**, *95*, 3435–3437.

- (8) Chase, M. W., Jr. *J. Phys. Chem. Ref. Data* **1998**, Monograph 9.
- (9) Albaret, T.; Finocchi, F.; Noguera, C. *J. Chem. Phys.* **2000**, *113*, 2238–2249.
- (10) Woodley, S. M.; Hamad, S.; Mejias, J. A.; Catlow, C. R. A. *J. Mater. Chem.* **2006**, *16*, 1927–1933.
- (11) Adamo, C.; Barone, V. *J. Chem. Phys.* **1998**, *108*, 664–675.
- (12) Perdew, J. P.; Chevary, J. A.; Vosko, S. H.; Jackson, K. A.; Pederson, M. R.; Singh, D. J.; Fiolhais, C. *Phys. Rev. B* **1992**, *46*, 6671–6687.
- (13) Perdew, J. P.; Chevary, J. A.; Vosko, S. H.; Jackson, K. A.; Pederson, M. R.; Singh, D. J.; Fiolhais, C. *Phys. Rev. B* **1993**, *48*, 4978.
- (14) Becke, A. D. *J. Chem. Phys.* **1993**, *98*, 5648–5651.
- (15) Hamprecht, F. A.; Cohen, A. J.; Tozer, D. J.; Handy, N. C. *J. Chem. Phys.* **1998**, *109*, 6264–6271.
- (16) Boese, A. D.; Martin, J. M. L.; Handy, N. C. *J. Chem. Phys.* **2003**, *119*, 3005–3014.
- (17) Frisch, M. J.; et al. Gaussian 03, Revision C.02, 2003; Gaussian, Inc.: Wallingford, CT, 2004.
- (18) Krishnan, R.; Binkley, J. S.; Seeger, R.; Pople, J. A. *J. Chem. Phys.* **1980**, *72*, 650–654.
- (19) McLean, A. D.; Chandler, G. S. *J. Chem. Phys.* **1980**, *72*, 5639–5648.
- (20) Wachters, A. J. *J. Chem. Phys.* **1970**, *52*, 1033–1036.
- (21) Hay, P. J. *J. Chem. Phys.* **1977**, *66*, 4377–4384.
- (22) Raghavachari, K.; Trucks, G. W. *J. Chem. Phys.* **1989**, *91*, 1062–1065.
- (23) Becke, A. D. *Phys. Rev. A* **1988**, *38*, 3098–3100.
- (24) Guest, M.; Bush, I. J.; van Dam, H.; Sherwood, P.; Thomas, J.; van Lenthe, J.; Havenith, R.; Kendrick, J. *Mol. Phys.* **2005**, *103*, 719–747.
- (25) TITAN is a set of electronic structure programs, written by T. J. Lee, A. P. Rendell, and J. E. Rice.
- (26) Hay, P. J.; Wadt, W. R. *J. Chem. Phys.* **1985**, *82*, 270–283.
- (27) Binkley, J. S.; Pople, J. A.; Hehre, W. J. *J. Am. Chem. Soc.* **1980**, *102*, 939–947.
- (28) Gordon, M. S.; Binkley, J. S.; Pople, J. A.; Pietro, W. J.; Hehre, W. J. *J. Am. Chem. Soc.* **1982**, *104*, 2792–2803.
- (29) Gordon, S.; McBride, B. J. Computer Program for Calculation of Complex Chemical Equilibrium Composition, Rocket Performance, Incident and Reflected Shocks and Chapman-Jouguet Detonations; Technical Report SP-273; NASA: Washington, DC, 1976.
- (30) Goodwin, D. G. An open source, extensible software suite for CVD process simulation. In *Chemical Vapor Deposition XVI and EUROCVD 14*; Allendorff, M.; Maury, F.; Teyssandier, F., Eds.; The Electrochemical Society: Pennington, NJ, 2003; Vol. 2003–08.
- (31) Hehre, W. J.; Ditchfield, R.; Radom, L.; Pople, J. A. *J. Am. Chem. Soc.* **1970**, *92*, 4796–4801.
- (32) Pople, J. A.; Luke, B. T.; Frisch, M. J.; Binkley, J. S. *J. Phys. Chem.* **1985**, *89*, 2198–2203.
- (33) Pople, J. A.; Curtiss, L. A. *J. Phys. Chem.* **1987**, *91*, 3637–3639.
- (34) Graham, D.; Beran, G.; Head-Gordon, M.; Christian, G.; Stranger, R.; Yates, B. *J. Phys. Chem. A* **2005**, *109*, 6762–6772.
- (35) McBride, B. J.; Gordon, S.; Reno, M. A. Coefficients for Calculating Thermodynamic and Transport Properties of Individual Species. Technical Report TM-4513; NASA: Washington, DC, 1993.
- (36) Wong, H. W.; Li, X. G.; Swihart, M. T.; Broadbelt, L. J. *J. Phys. Chem. A* **2004**, *108*, 10122–10132.
- (37) Hildenbrand, D. L. *High Temp. Mater. Sci.* **1996**, *35*, 151–158.